Relativistic four-component static-exchange approximation for core-excitation processes in molecules

Ulf Ekström* and Patrick Norman†
Department of Physics, Chemistry and Biology, Linköping University, SE-581 83 Linköping, Sweden

Vincenzo Carravetta‡
Istituto per i Processi Chimico-Fisici, Area della Ricerca del C.N.R., via G. Moruzzi 1, I-56124 Pisa, Italy
(Received 21 October 2005; published 2 February 2006)

A generalization of the static-exchange approximation for core-electron spectroscopies to the relativistic four-component realm is presented. The initial state is a Kramers restricted Hartree-Fock state and the final state is formed as the configuration-interaction single excited state, based on the average of configurations for $(n-1)$ electrons in n near-degenerate core orbitals for the reference ionic state. It is demonstrated that the static-exchange Hamiltonian can be made real by considering a set of time-reversal symmetric electron excitation operators. The static-exchange Hamiltonian is constructed at a cost that parallels a single Fock matrix construction in a quaternion framework that fully exploits time-reversal and spatial symmetries for the D_{2h} point group and subgroups. The *K*- and *L*-edge absorption spectra of H_2S are used to illustrate the methodology. The calculations adopt the Dirac-Coulomb Hamiltonian, but the theory is open ended toward improvements in the electron-electron interaction operator. It is demonstrated that relativistic effects are substantial for the *L*-edge spectrum of sulfur, and substantial deviations from the statistical 2:1 spin-orbit splitting of the intensity distribution are found. The average ratio in the mixed region is 1.54 at the present level of theory.

DOI: 10.1103/PhysRevA.73.022501 PACS number(s): 33.20.Rm

I. INTRODUCTION

In recent years, much effort has been devoted to the development of molecular electronic structure theory in the relativistic four-component realm. Several computational schemes that vary in accuracy and complexity have been formulated, ranging from the electron uncorrelated Hartree-Fock method to multiconfiguration self-consistent field and coupled-cluster approaches [1]. The work of adapting modern response theory so that it can be implemented in the four-component framework has also started, and, as far as linear response properties are concerned, we note the development of the linear polarization propagator in the relativistic random phase approximation (RPA) [2].

It is sometimes argued that the large number of electrons in heavy-atom compounds and the loss of electron spin symmetries make four-component methods computationally intensive and that more approximate approaches, such as the use of relativistic effective core potentials, are to be preferred in application work (rather than benchmarking work). Such a statement, however, must be qualified with respect to the property of interest. In this paper, we are concerned with a spectroscopy that directly probes the motions of the inner-shell electrons, and we argue that the fine structure of the spectra will contain details that require a fully relativistic treatment.

The electronic excitation spectrum is determined from the poles and the residues of the linear response function, and it can thus in principle be obtained from the linear response equation. In practice, however, this approach is limited to the lowest excitations from the valence shell due to the embedding of the core-excited states in the valence continuum. In addition, the RPA method is hampered by the missing electronic relaxation for excitations from the inner electronic shells. On the other hand, the remarkable improvements of x-ray spectroscopical investigations that has taken place at the third-generation synchrotron facilities and the capability of such experimental techniques of investigating important problems (in, for instance, surface chemistry) demand an adequate theoretical description of inner-shell spectra. For this purpose, a direct static-exchange (STEX) approach [3,4] was proposed for the calculation of core-ionization or core-excitation spectra (including decay processes), and, even though STEX can be seen, in one sense, as an approximation of the RPA, it outperforms the RPA approach due to the explicit account for the electronic relaxation in the presence of the core hole. The proposed *ab initio* method for the simulation of core-electron processes in molecules, has been widely and successfully employed for the interpretation of different x-ray spectroscopies [4–11].

It is evident that, by involving electrons of the inner shells, core-ionization and core-excitation processes are strongly affected by relativistic effects in molecules containing heavy elements, but this may be true also when only relatively light atoms are present. As is discussed in Sec. III, describing the *K*- and *L*-edge x-ray absorption spectra of H_2S, relativistic effects can be scalar in nature, i.e., essentially involving an energy shift of the spectrum (as observed at the *K* edge), but they can also be nonscalar in nature (as observed at the *L* edge). It has been pointed out by Kosugi [12] that high-resolution and sophisticated soft-x-ray mo-

*Electronic address: ulfek@ifm.liu.se
†Electronic address: panor@ifm.liu.se
‡Electronic address: carravetta@ipcf.cnr.it

lecular spectroscopies show that an accurate description of spin-orbit interaction, already in second-row elements, is essential for the interpretation of the finer details in inner-shell phenomena. In particular the *L*-shell absorption spectra of molecules containing sulfur or phosphorus can be difficult to analyze due to a complex interplay of core-valence-exchange interactions and spin-orbit interactions that may have comparable intensity. In molecules containing heavy elements, like, e.g., the technologically and biologically interesting organometallic compounds, spin-orbit effects may be present both in the hole as well as in the valence orbitals that are involved in the absorption process.

The main purpose of the present study is to create, by extension of the STEX approach to the relativistic four-component realm, a computational method that, in a rigorous way, treat relativistic effects in processes involving the excitation of core electrons in molecules. At the same time, this *ab initio* approach includes most of the other main effects that are important for core-electron processes, namely, electronic relaxation and core-valence exchange interaction.

In Sec. II A we give a brief summary of the main aspects of the nonrelativistic STEX method, while in Sec. II B the extension of the same approximation to the four-component framework and its implementation in the DIRAC program [13] will be outlined. In Sec. III we present the application of the proposed method to the calculation of the *K*- and *L*-edge near-edge x-ray absorption fine structure (NEXAFS) spectra of H_2S and discuss the main aspects of these spectra.

II. THEORY AND METHODOLOGY

A. The static-exchange method

The static-exchange method gives a complete excitation spectrum for excitations from one, or a few, core orbitals, and it takes orbital relaxation into account. More specifically, it corresponds to a singly excited configuration-interaction (CI) calculation with a core-hole optimized reference determinant. In this section, we will present a brief description of the STEX approximation and give the details of the modifications needed for its extension to the four-component realm.

Consider variations of an *N*-electron, closed-shell, reference determinant $|0\rangle$, generated by an anti-Hermitian excitation operator $\hat{T}=\Sigma_{A,I}X_{AI}\hat{q}_{AI}^{\dagger}-X_{AI}^{*}\hat{q}_{AI}$, where $\hat{q}_{AI}^{\dagger}=\hat{a}_{A}^{\dagger}\hat{a}_{I}$. Capital indices *A* and *B* are used for general unoccupied orbitals, whereas *I* and *J* are used for general occupied orbitals. With this parametrization the energy can be expanded in orders of the parameters as

$$E=\langle 0|e^{\hat{T}}\hat{H}_0e^{-\hat{T}}|0\rangle=E^{[0]}+E^{[1]}X+\frac{1}{2}X^{\dagger}E^{[2]}X+\cdots \quad (1)$$

where

$$E^{[0]}=\langle 0|\hat{H}_0|0\rangle,$$
$$E^{[1]}=\langle 0|[\hat{q}^{\dagger},\hat{H}_0]|0\rangle, \quad E^{[2]}=-\langle 0|[\hat{q},[\hat{q}^{\dagger},\hat{H}_0]]|0\rangle. \quad (2)$$

By optimizing the reference determinant so that $E^{[1]}$ vanishes, the random phase approximation excitation energies of the system are given by the solutions to the generalized eigenvalue problem [14],

$$\det[E^{[2]}-\omega S^{[2]}]=\det\left[\begin{pmatrix}A & B\\ B^{*} & A^{*}\end{pmatrix}-\omega\begin{pmatrix}1 & 0\\ 0 & -1\end{pmatrix}\right]=0, \quad (3)$$

where *A* describes the excitations and *B* contains the coupling of excitations and deexcitations generated by $\hat{T}$. The explicit forms of *A* and *B* are

$$A_{AI,BJ}=\langle 0|[-\hat{q}_{AI},[\hat{q}_{BJ}^{\dagger},\hat{H}_0]]|0\rangle = \delta_{IJ}F_{AB}-\delta_{AB}F_{IJ}^{*}+[(AI|JB)-(AB|JI)], \quad (4)$$

$$B_{AI,BJ}=\langle 0|[\hat{q}_{AI},[\hat{q}_{BJ},\hat{H}_0]]|0\rangle=[(AI|BJ)-(AJ|BI)], \quad (5)$$

where, if the electron-electron interaction in $\hat{H}_0$ is represented by the instantaneous Coulomb repulsion, the Fock operator is given by

$$F_{pq}=h_{pq}+\sum_{j=1}^{N}[(pq|jj)-(pj|jq)]. \quad (6)$$

Since the elements of the *B* matrix depend on the spatial overlap between core and virtual orbitals, they are in general small for core excitations. By applying the Tamm-Dancoff approximation, that is, neglecting the off-diagonal *B* block of $E^{[2]}$, the dimensionality of the problem can be reduced by a factor of 2. This approximation is well established for core excitations and results in negligible errors [3,4]. Furthermore, considering that core levels of different elements and/or different shells are, in general, well separated in energy, one can reduce the excitation space by only including excitations from those core orbitals that are expected to contribute in the desired energy region. This reduces the dimension of the Hessian, to a size where the *A* matrix can be explicitly constructed and diagonalized to get a full spectrum covering excitations both below (discrete) and above (continuum) the ionization threshold.

A point that is particular to the four-component relativistic RPA equation is the inclusion of excitations from electronic to positronic orbitals. The spectrum of the relativistic Fock operator is split into two branches, one set of "electronic" orbitals and another set of "positronic" orbitals, and, in the Dirac-Hartree-Fock (DHF) procedure the energy is simultaneously minimized with respect to the occupied electronic orbitals and maximized with respect to the positronic orbitals. In principle, the classification of orbitals as either electronic or positronic depends on the external potential [15,16], but, in weak molecular fields, it is determined by an energy splitting that is close to twice the electron rest energy. Up to this point it has been implicitly understood that the general unoccupied orbitals include virtual electronic orbitals as well as all positronic orbitals. It should be noted, however, that the electron-positron (*e-p*) transfer excitations in the RPA do not correspond to pair annihilation.

In the static-exchange approximation and other CI-based methods an explicit representation of the excited electronic states is formed by electronic excitations from a reference

wave function. In the no-pair approximation, it is therefore clear that the positronic orbitals must be excluded in the parametrization. If the *e-p* excitations are excluded in the electronic Hessian, we can argue that the *A* matrix corresponds to the CI singles Hamiltonian including determinants with holes in the included core orbitals,

$$\langle 0|[-\hat{q}_{AI},[\hat{q}^{\dagger}_{BJ},\hat{H}]]|0\rangle = \langle 0|\hat{q}_{AI}\hat{H}\hat{q}^{\dagger}_{BJ}|0\rangle - \delta_{IJ}\delta_{AB}E^{(0)} = H^{CI}_{AI,BJ} - \delta_{IJ}\delta_{AB}E^{(0)}. \quad (7)$$

This argument is true whether or not the reference determinant refers to a variationally optimized state, and, in analogy with the nonrelativistic case, the question is raised if there exists a better-suited reference determinant than the Hartree-Fock ground state. In fact the RPA is not suitable for core excitations since it neglects the large relaxation among the occupied orbitals in the excitation process. This in turn leads to a severe overestimation of the core-excitation energies (about 6 eV for the sulfur *L*-edge spectrum of H_2S). For highly excited states one expects that the final state resembles that of the ionized molecule together with the excited electron in a diffuse orbital. In the no-pair relativistic approximation the limiting electronic structure calculation is represented by separate-state multiconfiguration self-consistent field SCF optimizations of the molecular states with inclusion of *e-p* orbital rotations and a complete set of electron state transfer operators. The description of the ground and excited states is thus done with separate positronic states. The effect of these different embeddings is largely taken into account in our STEX approach, where the final state is formed as a single excited configuration-interaction state based on a separately optimized core-ionized reference state. The procedure also allows us to use the same reference state for all excitations from the same set of core orbitals. The set of core orbitals is chosen to include spin orbitals in a narrow energy range such as, e.g., the two $1s$, the two $2p_{1/2}$, or the four $2p_{3/2}$ spin orbitals, or the entire $2p$ shell. For a given set of n core spin orbitals, the ionized reference state is formed and optimized as the average of configurations for $(n-1)$ electrons in those orbitals. This approach overestimates the relaxation energy due to the neglect of screening from the excited electron, but the size of errors is greatly reduced as compared to the random-phase approximation.

After the STEX states have been formed by diagonalizing the *A* matrix the transition matrix elements are determined. Since the STEX states are not, in general, orthogonal to the Hartree-Fock ground state, a cofactor ($\mathcal{C}$) expansion is used. The overlap between two determinant wave functions $\langle\Psi|\Phi\rangle$ is given by the determinant of the overlap matrix *S*, and it follows that the transition matrix element between two nonorthogonal determinants for a one-electron operator $\hat{\Omega} = \sum_{k=1}^{N}\hat{\omega}_k$ can be written as

$$\langle\Psi|\hat{\Omega}|\Phi\rangle = \sum_{I,J}\langle\psi_I|\hat{\omega}|\phi_J\rangle\mathcal{C}_{IJ}S. \quad (8)$$

The nonorthogonality between initial and final states is an unphysical feature common to all methods based on separate state calculations. It introduces a gauge dependency in the calculation of the transition matrix elements, but, in practice, the overlap between the ground state and a core-excited state is rather small and can be considered to introduce negligible errors.

B. Implementation of the four-component STEX method

The electronic four-component molecular Hamiltonian has the same form as the nonrelativistic counterpart, and it can be written as

$$\hat{H} = \sum_{i=1}^{N}\hat{h}(i) + \sum_{i>j}\hat{g}(i,j), \quad (9)$$

where $\hat{h}$ is the one-electron Dirac Hamiltonian and $\hat{g}(i,j)$ represents the electron-electron interaction. If, for $\hat{g}$, one substitutes the instantaneous Coulomb repulsion, the Dirac-Coulomb Hamiltonian is obtained, and full account is made of the spin–own-orbit interactions whereas current-current interactions are left out. The calculations in the present work adopt this approximation, but the formulation of the STEX method is not restricted to this situation.

The Fock operator [Eq. (6)] for a closed-shell system is time-reversal symmetric. For this reason, the orbital energies are doubly degenerate, and the corresponding spinors of each pair are related through the operation of time reversal, or the Kramers operator $\hat{K}$. Arranging the four components of a one-electron spinor as

$$\psi_i(\mathbf{r}) = \begin{pmatrix}\psi_i^{L\alpha}\\ \psi_i^{S\alpha}\\ \psi_i^{L\beta}\\ \psi_i^{S\beta}\end{pmatrix} = \begin{pmatrix}\psi_i^{\alpha}\\ \psi_i^{\beta}\end{pmatrix}, \quad (10)$$

the Kramers operator is defined by its action on a spinor according to

$$\hat{K}\psi_i(\mathbf{r}) = \psi_{\bar{i}}(\mathbf{r}) = \begin{pmatrix}-\psi_i^{\beta *}\\ \psi_i^{\alpha *}\end{pmatrix}, \quad (11)$$

where we have introduced the overbar notation on the indices to indicate Kramers partners. In the following discussion we will use upper-case indices when referring to a general spinor, while lower-case indices, with and without overbar, are reserved for Kramers pairs. We briefly note that $\hat{K}^2\psi_i = \psi_{\bar{i}\bar{i}} = -\psi_i$. In developing working formulas it is advantageous to consider operators of well-defined time-reversal symmetry ($t=+/-$ for symmetric and antisymmetric operators, respectively) so that $\hat{K}\hat{\Omega}^t\hat{K}^{-1} = t\hat{\Omega}^t$, because, for time-reversal-symmetric wave functions, the expectation value of such operators is

$$\langle 0|\hat{\Omega}^t|0\rangle = t\langle 0|\hat{\Omega}^t|0\rangle^*. \quad (12)$$

As a consequence of this fact, the expectation value of a time-reversal-symmetric operator is purely real, which allows us to use real algebra for its matrix representation. In a second-quantization formalism, the time-reversal operation

is introduced according to $\hat{K}\hat{a}_a^\dagger\hat{a}_i\hat{K}^{-1}=\hat{a}_{\bar{a}}^\dagger\hat{a}_{\bar{i}}$ and $\hat{K}\hat{a}_a^\dagger\hat{a}_{\bar{i}}\hat{K}^{-1}=-\hat{a}_{\bar{a}}^\dagger\hat{a}_i$.

We will now exploit the time-reversal symmetry of the reference state in the STEX calculation. Due to the properties of the two-electron integrals and the Fock matrix under time reversal, the following relations exist between the elements of the A matrix given in Eq. (4):

$$A_{ai,bj}=A^*_{\bar{a}\bar{i},\bar{b}\bar{j}},\quad A_{ai,\bar{b}\bar{j}}=A^*_{\bar{a}\bar{i},bj},\quad A_{\bar{a}i,bj}=-A^*_{a\bar{i},\bar{b}\bar{j}},$$
$$A_{a\bar{i},bj}=-A^*_{\bar{a}i,\bar{b}\bar{j}}. \tag{13}$$

The A matrix is in general complex, but by choosing the parametrization in terms of time-reversal-symmetric excitation operators it can be made real. A unitary transformation of the excitation operators that satisfies this condition is

$$\{\hat{E}^{t\dagger}_{ai},\hat{E}^{u\dagger}_{\bar{a}i}\}=\frac{1}{\sqrt{2}}\{\theta_t(\hat{q}^\dagger_{ai}+t\hat{q}^\dagger_{\bar{a}\bar{i}}),\theta_u(\hat{q}^\dagger_{\bar{a}i}-u\hat{q}^\dagger_{a\bar{i}})\}, \tag{14}$$

with t and u both taking on signs + and −. The phase θ_α is defined as $\theta_+=1,\theta_-=i$. In this picture $\hat{E}^{+\dagger}_{ai}$ generates singlet excitations in the nonrelativistic limit when all spin orbitals with unbarred indices are chosen to be spin eigenfunctions with identical spin. The other three "triplet" operators are usually excluded from the excitation space in a nonrelativistic calculation since they do not contribute to the final oscillator strength distribution. In a relativistic calculation they are, however, necessary because spin-orbit coupling breaks spin conservation during the excitation process. With inclusion of the full transformed excitation manifold, the elements of the STEX Hamiltonian become

$$A^{tu}_{ai,bj}=\langle 0|[-\hat{E}^t_{ai},[\hat{E}^{u\dagger}_{bj},\hat{H}_0]]|0\rangle$$
$$=\frac{1}{2}t\theta_t\theta_u(A_{ai,bj}+tuA^*_{ai,bj}+uA_{ai,\bar{b}\bar{j}}+tA^*_{ai,\bar{b}\bar{j}}), \tag{15}$$

$$A^{tu}_{ai,\bar{b}\bar{j}}=\langle 0|[-\hat{E}^t_{ai},[\hat{E}^{u\dagger}_{\bar{b}\bar{j}},\hat{H}_0]]|0\rangle$$
$$=\frac{1}{2}t\theta_t\theta_u(A_{ai,\bar{b}\bar{j}}+tuA^*_{ai,\bar{b}\bar{j}}-uA_{ai,bj}-tA^*_{ai,bj}), \tag{16}$$

$$A^{tu}_{\bar{a}i,\bar{b}\bar{j}}=\langle 0|[-\hat{E}^t_{\bar{a}i},[\hat{E}^{u\dagger}_{\bar{b}\bar{j}},\hat{H}_0]]|0\rangle$$
$$=\frac{1}{2}t\theta_t\theta_u(A^*_{a\bar{i},\bar{b}\bar{j}}+tuA_{a\bar{i},\bar{b}\bar{j}}-tA_{a\bar{i},\bar{b}j}-uA^*_{a\bar{i},\bar{b}j}), \tag{17}$$

$$A^{tu}_{\bar{a}i,bj}=\langle 0|[-\hat{E}^t_{\bar{a}i},[\hat{E}^{u\dagger}_{bj},\hat{H}_0]]|0\rangle$$
$$=\frac{1}{2}t\theta_t\theta_u(-tuA_{a\bar{i},\bar{b}\bar{j}}-A^*_{a\bar{i},\bar{b}\bar{j}}-tA_{a\bar{i},bj}-uA^*_{a\bar{i},bj}). \tag{18}$$

It is clear that, since the matrices A and A^{tu} are related by a unitary transformation, their sets of eigenvalues are identical, and the eigenvectors correspond to identical states, and we will choose to construct and diagonalize A^{tu} because it is real.

The STEX Hamiltonian is constructed by combining Eqs. (15)–(18) with Eq. (4). The matrix elements on the diagonal, i.e., $A_{AI,AI}$, include the difference in hole and electron orbital energies in addition to the difference in exchange and Coulomb interactions between the hole and electron orbitals, whereas the latter contribution is the sole contributor to the off-diagonal elements of the Hamiltonian. The necessary exchange and Coulomb integrals are obtained by contracting atomic orbital integrals over suitably chosen one-electron hole-orbital transition-density matrices. If N_{hole} denotes the number of hole orbitals included in the construction of the ionized reference state, then $2N_{\mathrm{hole}}(N_{\mathrm{hole}}+1)$ such transition-density matrices are needed. However, since the number of hole orbitals is small the atomic-orbital contraction of the densities can be performed in one batch, and the cost of the method thus parallels that of a single Fock matrix construction with the possibility to use the existing routines in a program for DHF calculations—the DIRAC [13] program in the present context.

For an efficient implementation it is necessary to exploit the time-reversal and spatial symmetries in the two-electron integral evaluation. For this reason we symmetrize the density matrices with respect to time reversal. The molecular point group is automatically exploited in the integral evaluation by the quaternion symmetry scheme [17] of the DIRAC program. In this representation the spinors are written in quaternion form according to

$$\psi_i=\begin{pmatrix}\psi_i^\alpha\\ \psi_i^\beta\end{pmatrix}\leftrightarrow\begin{pmatrix}\mathrm{Re}\ \psi_i^\alpha+\mathrm{Im}\ \psi_i^\alpha\check{1}\\ -\mathrm{Re}\ \psi_i^\beta\check{J}+\mathrm{Im}\ \psi_i^\beta\check{k}\end{pmatrix}\leftrightarrow {}^Q\psi_i=\psi_i^\alpha-\psi_i^{\beta*}\check{J}, \tag{19}$$

where $\check{\imath}$, $\check{J}$, and $\check{k}$ are the three anticommuting quaternion units, satisfying $\check{\imath}^2=\check{J}^2=\check{k}^2=\check{\imath}\check{J}\check{k}=-1$, and the operation of time reversal is given by $\hat{K}\psi\leftrightarrow-\check{J}\,{}^Q\psi_i$. The time-reversal-symmetric density matrices that we need to consider in order to determine the matrix elements $A_{AI,BJ}$ are

$$|i\rangle\langle j|+|\bar{i}\rangle\langle\bar{j}|\leftrightarrow {}^Q\psi_i\,{}^Q\psi_j^\dagger, \tag{20}$$

$$\check{\imath}(|i\rangle\langle j|-|\bar{i}\rangle\langle\bar{j}|)\leftrightarrow {}^Q\psi_i\check{\imath}\,{}^Q\psi_j^\dagger, \tag{21}$$

$$|i\rangle\langle\bar{j}|-|\bar{i}\rangle\langle j|\leftrightarrow {}^Q\psi_i\check{J}\,{}^Q\psi_j^\dagger, \tag{22}$$

$$\check{\imath}(|i\rangle\langle\bar{j}|+|\bar{i}\rangle\langle j|)\leftrightarrow {}^Q\psi_i\check{k}\,{}^Q\psi_j^\dagger. \tag{23}$$

These transition-density matrices are transformed to the atomic-orbital basis and used to contract the set of two-electron integrals. Computational cost and memory storage reductions in this step due to spatial symmetry in the system will parallel other parts of the program, and we refer to the discussion on reductions to complex or real algebra that is found in the work of Saue and Jensen [17]. Based on the symmetries of the excited states, it is also possible to employ the quaternion symmetry scheme to perform a block diagonalization of the STEX Hamiltonian, but the performance gain in this step is insignificant compared to the overall computational cost.

The final step in the calculation involves the diagonalization of the STEX Hamiltonian, and the oscillator strengths are then computed from the eigenvectors through Eq. (8). Above the core-ionization threshold the true absorption spectrum is continuous, and, in this region, a method such as Stieltjes imaging can be used to obtain a realistic spectrum from the discrete STEX spectrum.

III. APPLICATION TO THE *K*- AND *L*-EDGE NEXAFS OF H_2S

The features of the proposed four-component static exchange approach are demonstrated by the calculation of the NEXAFS spectra of the sulfur *K* and *L* edges of H_2S. Sulfur is a relatively light element, and, as such, we expect significant relativistic effects to be found in the core only; a scalar-relativistic contraction of the 1*s* orbital and a spin-orbit splitting of the 2*p*-shell.

In the C_{2v} point group, a H-S bond length of 1.328Å and a H-S-H bond angle of 92.2° were used for the calculations, in accordance with the experimental molecular structure [18].

A decontracted basis set was used, with the exponents for the core and valence taken from the augmented triple-ζ basis set of Woon and Dunning (aug-cc-pVTZ) [19]. This basis set was further augmented with diffuse functions with exponents taken from a geometrical series with a factor of 1.6 (the most diffuse exponent was equal to 0.000 850 a.u.). The sulfur core region was supplemented with two even-tempered tight functions, with the factor taken from the two tightest *p* functions in the aug-cc-pVTZ set. Only *s* functions were included for the hydrogen atoms, because the large basis set on the sulfur atom was found to account for the polarization of the hydrogen as well. The final large component basis set included $[31s31p28d10f3g]$ and $[4s]$ for sulfur and hydrogen, respectively. All calculations were carried out with a locally modified version of the DIRAC program [13], with the small component basis set generated from the restricted kinetic balance condition. The oscillator strengths presented are calculated in the dipole length gauge.

A. Sulfur *K*-edge spectrum

The STEX calculation for the sulfur *K* edge is preceded by self-consistent field optimizations of the molecular ground state and the core-ionized states formed as the average of configurations with a hole in one of the two sulfur 1*s* orbitals. The main relativistic effect for the *K* edge is expected to be the scalar-relativistic lowering of the 1*s*-orbital energy and the contraction of the hole orbitals from which one could anticipate an effect on the oscillator strengths. In order to get an estimate of the orbital contraction we have determined the orbital expectation value $\langle 1s|\hat{r}^2|1s\rangle$; the results are 0.012 51 and 0.012 41 a.u. at the nonrelativistic and relativistic levels of theory, respectively. It is clear that the contraction is very small, and the effect on the oscillator strengths is also negligible (0.6% for the strong B_2 transition, which is the fourth state in Table I).

TABLE I. Excitation energies (eV) and oscillator strengths for the sulfur *K*-edge spectrum of H_2S below 2479.5 eV. Four-component relativistic (REL) STEX results are compared with the corresponding nonrelativistic (NR) results.

State	E_{REL}	f_{0n}^{REL} (units of 10^{-3})	$E_{\mathrm{REL}}-E_{\mathrm{NR}}$	f_{0n}^{NR} (units of 10^{-3})
B_2	2475.81	0.006	8.39	0
A_1	2475.89	0.016	8.41	0
A_1	2475.96	0.994	8.39	1.005
B_2	2476.05	4.347	8.41	4.374
B_2	2477.76	0.084	8.41	0.086
A_1	2477.82	0.381	8.40	0.382
B_1	2477.91	0.712	8.40	0.715
A_1	2478.15	0.541	8.41	0.545
A_1	2478.55	0.011	8.40	0.011
A_1	2478.72	0.001	8.40	0.001
B_2	2478.89	0.216	8.40	0.216
B_2	2479.04	0.030	8.40	0.030
A_1	2479.05	0.123	8.40	0.123
B_1	2479.08	0.234	8.40	0.235
A_1	2479.12	0.175	8.40	0.176
A_1	2479.29	0.003	8.40	0.003
B_1	2479.37	0.002	8.40	0.002
A_1	2479.46	0.092	8.40	0.092

The ΔSCF value of the 1*s* ionization potential is 2480.2 eV at the four-component Hartree-Fock level, i.e., a shift of 8.40 eV compared to the nonrelativistic value of 2471.8 eV. Besides this overall shift there are no significant relativistic effects on the *K* edge sulfur spectrum, for instance, the integrated intensity from triplet states adds to less than 0.3% of the total oscillator strength below the ionization threshold (see Fig. 1). Below 2479.5 eV there are only two triplet states that have oscillator strengths larger than 10^{-6}. These two states are reported as the first two states in Table I, but we remind the reader that other triplet states are left out

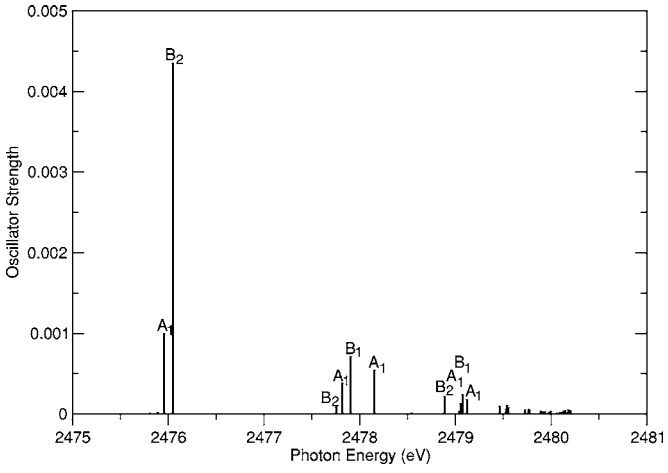

FIG. 1. Sulfur *K*-edge x-ray absorption spectrum determined at the four-component static-exchange level of theory.

in the report. The experimental ionization potential is 2478.3 eV [20].

Hence, the K edge of H_2S is fully described at the scalar relativistic level of theory, or alternatively the scalar relativistic energy shift can be added by hand to a nonrelativistic calculation.

B. Sulfur L-edge spectrum

1. X-ray photoemission spectrum

We now turn our attention to the sulfur L edge of H_2S, where nonscalar relativistic effects are known to play a major role due to the spin-orbit effects in the $2p$ shell. In this section we will focus on the electronic ionization potentials and in the subsequent section we discuss the fine structure of the absorption spectrum. The $2p$ orbital energies are split by the spin-orbit coupling into two levels that correspond to the two $2p_{1/2}$ and the four $2p_{3/2}$ orbitals. A close inspection reveals a further splitting of the $2p_{3/2}$ level due to the molecular field, so there are all in all three energy levels in the sulfur $2p$ shell in H_2S.

The calculation of the sulfur x-ray photoemission spectrum rests on the SCF optimizations of the ground state and the core-ionized state with one electron missing in the $2p$ shell. In the optimization of the core-ionized state one optimizes three separate average-of-configurations states based on one electron in the each of the three doubly degenerate energy levels, respectively. Although the spin-orbit splitting of $2p_{1/2}$ and $2p_{3/2}$ can be estimated directly from the orbital energies of the ground state ($\Delta\epsilon$), a more appropriate choice is to determine the energy differences between the three core-ionized states (ΔSCF). The ΔSCF values can be directly compared to x-ray photoemission spectroscopy (XPS) measurements. For H_2S we determine the ΔSCF ionization potentials to be 171.24, 169.98, and 169.96 eV, respectively, and, for the average spin-orbit splitting between the $2p_{1/2}$ and the two $2p_{3/2}$ levels, we thus obtain a value of 1.27 eV ($\Delta\epsilon$ = 1.32 eV). This is an overestimation of the spin-orbit splitting by 0.07 eV, as compared to the experimental XPS value of 1.20 eV [21]. This discrepancy is partly due to the lack of spin–other-orbit interactions in the Dirac-Coulomb Hamiltonian. The inclusion of spin–other-orbit interactions by inclusion of the Breit operator in the Hamiltonian would result in a decrease of the spin-orbit splitting. The molecular field splitting of the $2p_{3/2}$ levels is known to be underestimated at the nonrelativistic Hartree-Fock level, due to electron correlation effects, and we confirm this also for the DHF case. We obtain a ΔSCF splitting of 27 meV (the $\Delta\epsilon$ splitting is 23 meV), as compared to the experimental result of 106 meV [22]. The nonrelativistic electron-correlated calculation of Ref. [23] gives a splitting of 108 meV.

2. Near-edge x-ray-absorption fine structure

The NEXAFS spectra are determined with the STEX method as outlined in Sec. II A. Before entering a discussion about the physical characteristics of the relativistic sulfur L-edge NEXAFS spectrum for H_2S we will, in the two paragraphs below, first address two computational issues, namely, the choice of core-ionized reference state and channel interaction.

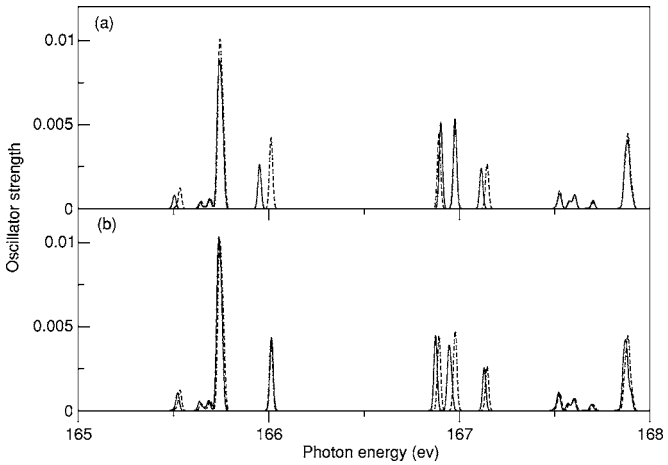

FIG. 2. The effects of channel coupling (exchange interaction) and reference-state optimization on the mixed region of the sulfur L-edge spectrum of H_2S. (a) Full channel interaction (solid line) is compared to the added spectrum (dashed line) of one part with excitations from $2p_{1/2}$ and one with excitations from $2p_{3/2}$. (b) A single reference state (dashed line) with five electrons in the six $2p$ orbitals is compared to the use of two separate reference states (solid line) optimized for $2p_{1/2}$ and $2p_{3/2}$, respectively. Both these spectra exclude the channel coupling between the $2p_{1/2}$ and $2p_{3/2}$ orbitals.

In the optimization of the core-ionized state there are two possible strategies, either one optimizes a single average of configurations with five electrons in six orbitals or one optimizes two separate averages of configurations with one electron in $2p_{1/2}$ and three electrons in $2p_{3/2}$, respectively. In Fig. 2(b) we compare the NEXAFS spectra in the mixed region for, on the one hand, a single core-ionized reference state and, on the other hand, two separate-state optimized reference states. In general the differences in the two resulting spectra are small, although a small decrease in the excitation energies from the $2p_{1/2}$ shell are noticed for the separate-state optimization case (see the three absorption peaks around 167 eV). In the STEX approach, the choice of a common core-ionized reference state for the formation of all the corresponding core-excited states is really based on the fact that this recipe provides final states that well correspond to the true ones. In cases of near-degenerate orbital levels, as the $2p_{1/2}$ and $2p_{3/2}$ levels, it becomes difficult to argue whether one should treat them separately or not. For the sulfur L-edge spectrum, the differences in final spectra are so small that we have adopted the more straightforward of the two alternatives, namely, the one-step five-in-six approach. Moreover, the formation of the STEX Hamiltonian with inclusion of a small subset of all orbital excitation operators is warranted due to the large separation in energies between the included hole orbitals and others, and, in this respect, it is not reasonable to treat excitations from the $2p$ sublevels separately.

In the two spectra shown in Fig. 2(b), we have calculated two separate spectra based on excitations from the $2p_{1/2}$ and the $2p_{3/2}$ orbitals, respectively, and added the two afterward.

TABLE II. Excitation energies (eV) and oscillator strengths for the sulfur L-edge spectrum of H_2S below 169.55 eV. States with oscillator strengths $f_{0n} > 0.0005$ are included. The percentage contributions of each hole orbital to the excited states are reported, and these are defined as the sum of the squares of the corresponding elements of eigenvectors of the STEX Hamiltonian.

		$2p_{3/2}^{-1}$			$2p_{1/2}^{-1}$		
State	E	f_{0n} (units of 10^3)	$2p_{3/2}$ (%)	E	f_{0n} (units of 10^3)	$2p_{1/2}$ (%)	ΔE
B_2	165.50	0.79	98.4				
B_1	165.69	0.54	99.9				
B_2	165.73	6.23	99.9	166.90	5.10	97.8	1.17
A_1	165.75	4.91	99.9	166.97	3.54	99.5	1.22
B_1	165.76	3.33	99.8	166.98	2.10	99.2	1.22
A_1	165.95	2.61	97.3	167.11	2.40	95.1	1.16
A_1	167.61	0.76	99.8				
B_1	167.87	2.62	99.7	169.13	1.04	10.2	1.26
B_1	167.89	3.46	99.9	169.14	2.08	83.2	1.25
B_2	167.90	0.84	99.7	169.14	0.62	80.6	1.24
B_2	168.30	1.64	100.0	169.55	0.85	81.5	1.25
A_1	168.30	1.00	99.9				
B_2	168.37	1.41	100.0				
B_1	168.40	0.75	100.0				
A_1	168.44	1.01	100.0				
B_1	168.47	0.55	100.0				
B_1	168.87	1.17	96.9				
B_2	169.06	0.71	99.8				
B_2	169.07	0.76	99.2				
A_1	169.10	0.62	99.0				
B_1	169.31	0.75	99.8				

The reason for this is that we wanted to exclude channel interactions in the comparison of choices of reference states, and, instead, we give explicit account of the effects of channel interactions in Fig. 2(a). Channel interaction implies of course that there can be no exact division of the final states as arising from excitations from *either* the electronic $2p_{1/2}$ *or* $2p_{3/2}$ states. However, the spin-orbit splitting of the two orbitals amounts to about 1.2 eV for sulfur so in practice there is little mixing of the respective excitation amplitudes in the eigenvectors of the STEX Hamiltonian. Nevertheless, the effect on the spectra is significant. With inclusion of channel interactions, we observe an increase in the $2p_{3/2}$-$2p_{1/2}$ energy split, as well as a transfer of absorption intensity to the $2p_{1/2}$ states. Using a nonrelativistic way of speaking, one might say that the $2p_{1/2}$ states become more singlet in nature due to the exchange interaction (see the more complete discussion below). Clearly, full channel interaction is and should be used in the calculations of L-edge spectra, and the single core-ionized reference state suitable for a description of the complete spectrum is an average of configurations with five electrons in six orbitals. All results discussed below are obtained with this approach.

The excitation energies and oscillator strengths of the most important states in the energy region of 165.5–169.5 eV are listed in Table II, and the corresponding theoretical absorption spectrum is depicted in Fig. 3. The first spectral feature consists of excitations from the $2p$ shell into the lowest virtual orbitals, namely, $6a_1$ and $3b_2$. Since spin-orbit coupling is negligible for the valence orbitals in H_2S, we use the nonrelativistic labeling of these orbitals. Using the orbitals of the ion, this part of the spectrum can be completely interpreted as excitations from the six core orbitals into $6a_1$ and $3b_2$, since the higher virtual orbitals have

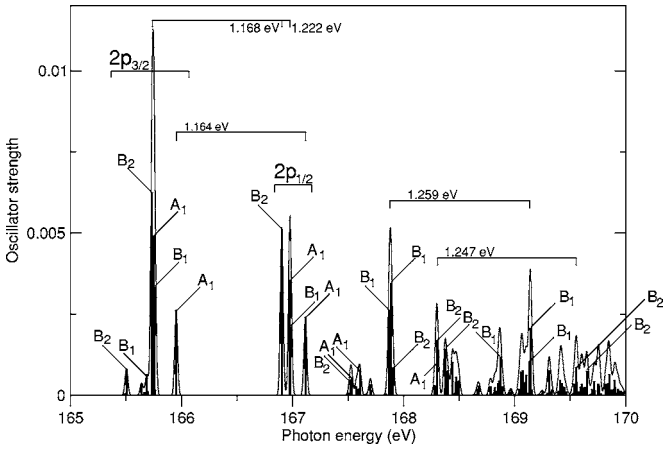

FIG. 3. Sulfur L-edge x-ray absorption spectrum determined at the four-component static-exchange level of theory. The spectrum displays the mixed region (165.0–167.3 eV) and the Rydberg region (167.5–170.0 eV). Spin-orbit splittings are given for selected states.

negligible weight for the excited states in this energy region. The hole in the core makes the $6a_1$ and $3b_2$ orbitals strongly bound and quite well separated in energy from others, which is the reason there is very little mixture from other virtual orbitals in the formation of the excited states. In the ionic state, the $3b_2$ orbital energy is actually below that of the $6a_1$ orbital (by 50 meV), due to the polarization of the occupied orbitals in the vicinity of the core hole. When the electrons move closer to the hole the $6a_1$ virtual orbital density is pushed away from this region. For the $3b_2$ orbital this effect is less pronounced because this orbital has a node on the sulfur atom. Thus the lowering of the orbital energies due to the core hole is larger for $3b_2$, but it is the final spectrum that is to be accounted for, and in this respect these orbital eigenvalues have only limited predictive power.

The six hole orbitals and the four virtual orbitals give rise to a collection of 24 excited states, six of which would appear as singlets in a nonrelativistic treatment. With relativity taken into account, there are 18 dipole-allowed excited states, six in each of the irreducible representations A_1, B_1, and B_2. The energy separation of the virtual orbitals is small, and the excited states will have contributions from a mixture of the $6a_1$ and $3b_2$ virtual orbitals. The energy separation of the hole orbitals, on the other hand, is larger and the final state is in most cases characterized as either a $2p_{3/2}^{-1}$ or a $2p_{1/2}^{-1}$ state, but a certain channel interaction exists. The amount of channel interaction for a given final state can be calculated from the eigenvectors of the STEX Hamiltonian, and we show these percentage contributions from the hole orbitals for the lowest states in Table II. For some states the mixing is very strong, making a labeling in terms of hole orbitals difficult. In particular the $2p_{1/2}^{-1}$ states tend to mix with higher excited $2p_{3/2}^{-1}$ states, as is observed around 169.13 eV.

At the experimental ground-state geometry, the lowest $^1B_2$ and $^1A_1$ states in the L-edge spectrum are almost degenerate in the STEX calculation ($2p_{3/2}^{-1}$ states numbers three and four in Table II). Indeed a crossing of the two potential energy surfaces was found in nonrelativistic multiconfiguration SCF work by Naves de Brito and Ågren [24]. The STEX reference state is optimized completely in the absence of the excited electron, which causes some overscreening and exaggerates the lowering of the $^1B_2$ state, so some discrepancy is to be expected. A complete analysis of the complicated vibrational structure of these states is beyond the scope of the present paper.

Based on earlier theoretical work [25–27], an analysis of the experimental NEXAFS spectrum has been performed by Hudson *et al.* [22]. In this analysis the apparent spin-orbit splitting was found to be varying, from 1.112 eV in the mixed valence-Rydberg region to 1.204 eV in the Rydberg region, due to the different exchange interaction between the excited electron and the hole in the $2p_{1/2}$ and the $2p_{3/2}$ orbitals. The combination of exchange and spin-orbit interactions is particularly important for second-row elements like sulfur, where the two effects are of comparable strength [12]. In this way the L-edge spectrum generally contains more information about the excited states than the K-edge spectrum. With a fully relativistic approach, however, we are in a position to address the differences in apparent spin-orbit splitting that may occur within the mixed valence-Rydberg region itself. Since the $6a_1$ orbital of H_2S has a much larger charge density (and different nodal structure) in the sulfur core region as compared to the $3b_2$ orbital, we expect a different apparent spin-orbit splitting also for the different states in the mixed region (due to different hole–excited electron exchange interaction). The splitting between the intense B_2 states (excitations to the $3b_2$ orbital) is 1.168 eV, while the splitting between the intense A_1 states (involving only $6a_1$) is 1.222 eV (see Fig. 3). In the Rydberg region STEX gives a splitting of 1.25 eV, which is close to the ΔSCF value of 1.27 eV that was given in Sec. III B 1.

The coupling between the different excitation channels, represented by the off-diagonal blocks of the STEX Hamiltonian, is of importance for the fine structure of the absorption spectrum. In the present case, the channel coupling contains exchange interaction between the $2p_{1/2}^{-1}$ and $2p_{3/2}^{-1}$ states, and this leads to a small *increase* in the apparent spin-orbit splittings. On the other hand, we note that the exchange effects within the respective channels will reduce the apparent spin-orbit splittings due to a larger increase of the $2p_{3/2}^{-1}$ absorption energies as compared to those for the $2p_{1/2}^{-1}$ states, and the inter- and intrachannel exchange interactions thus cancel each other to some extent. Another effect of exchange interactions is that part of the absorption intensity is transferred from the $2p_{3/2}^{-1}$ states to the $2p_{1/2}^{-1}$ states [see Fig. 2(a)]. The reason is that the exchange interaction, which favors parallel spins, gives the higher-energy state more of a singlet character. In the limit of a small spin-orbit splitting the hole-excited electron-exchange interaction is the dominant force, and the states separate completely into singlet and triplet states, with all the oscillator strength collected by the singlet states. Because of the interplay between exchange interaction and spin-orbit interaction, the oscillator strengths can deviate from the statistical ratio of 2:1 corresponding to a null exchange interaction. In the present calculations, it is possible to assign each of the mixed region excitations as originating from either the $2p_{1/2}$ orbitals or some combination of the two $2p_{3/2}$ orbitals. In this way the total intensity ratios for excitations from the two $2p_{3/2}$ orbitals or the single $2p_{1/2}$ orbital, in the mixed region, were determined to be 1.34 (A_1 states), 1.87 (B_1), and 1.42 (B_2), giving an average ratio of 1.54; the experimental ratios are given in Ref. [22] as ranging from 1.2 to 1.8. However, the large vibrational broadening in the experimental spectrum made the assignment difficult, and, because of this fact, we do not make a direct comparison of our theoretical electronic spectrum with the experimental one. Similar deviations of the value of the intensity ratio from the statistical value of 2 have been observed in the NEXAFS spectrum of SO_2 at the sulfur L edge [12].

IV. CONCLUSIONS

A development and implementation of the four-component static-exchange approximation is presented. With the analysis of the L-edge spectrum of H_2S we show that the method enables calculations of experimental observables that are inaccessible to nonrelativistic methods, and, considering the richness in details in L-edge spectra in general, this development should play an important role for the analysis of

experimental spectra. It is demonstrated that the spin-orbit splitting of the sulfur $2p_{1/2}$ and $2p_{3/2}$ energy levels as well as the intensity distributions are sensitive to the excited state, and thus the molecular environment. Since four-component methods treat relativistic effects in both the core and valence regions, the proposed four-component static-exchange method can be used for the analysis of molecular materials containing heavy elements in which valence spin-orbit coupling is important.

The computational scaling of the four-component static-exchange method is the same as the underlying Hartree–Fock program, and it imposes no additional limitations to the system size or the handling of time-reversal and spatial symmetries. The construction of the static-exchange Hamiltonian is formulated as contractions of one-electron transition-density matrices with atomic orbitals in a way that parallels a regular Fock matrix construction. Existing routines in the program are used for this purpose and the methodology is thus open ended toward general improvements in the code such as, for instance, handling of two-electron integrals or treatment of current-current interactions in the Hamiltonian. The static-exchange method as described in this paper has been implemented in the DIRAC program[13].

ACKNOWLEDGMENTS

The authors acknowledge financial support from the European Research and Training Network "Molecular Properties and Molecular Materials" (MOLPROP), Contract No. HPRN-CT-2000-00013, and computing time from National Supercomputer Centre (NSC), Sweden.

[1] L. Visscher, in *Relativistic Electronic Structure Theory: Part 1, Fundamentals*, edited by P. Schwerdtfeger (Elsevier, Amsterdam, 2002), Chap. 6.
[2] T. Saue and H. J. Aa. Jensen, J. Chem. Phys. **118**, 522 (2003).
[3] H. Ågren, V. Carravetta, O. Vahtras, and L. Petterson, Chem. Phys. Lett. **222**, 75 (1994).
[4] H. Ågren, V. Carravetta, O. Vahtras, and L. Petterson, Theor. Chem. Acc. **97**, 14 (1997).
[5] O. Plachkevytch, V. Carravetta, O. Vahtras, and H. Ågren, Chem. Phys. **232**, 49 (1998).
[6] O. Plachkevytch, T. Privalov, H. Ågren, V. Carravetta, and K. Ruud, Chem. Phys. **260**, 11 (2000).
[7] V. Carravetta, H. Ågren, O. Vahtras, and H. J. Aa. Jensen, J. Chem. Phys. **113**, 7790 (2000).
[8] K. Kaznacheyev, A. Osanna, C. Jacobsen, O. Plashkevych, O. Vahtras, H. Ågren, V. Carravetta, and A. P. Hitchcock, J. Phys. Chem. **113**, 7790 (2000).
[9] G. Iucci, V. Carravetta, P. Altamura, M. V. Russo, G. Paolucci, A. Goldoni, and G. Polzonetti, Chem. Phys. **302**, 43 (2004).
[10] M. Piancastelli, V. Carravetta, I. Hjelte, A. De Fanis, K. Okada, N. Saito, M. Kitajima, H. Tanaka, and K. Ueda, Chem. Phys. Lett. **399**, 426 (2004).
[11] M. Alagia, C. Baldacchini, M. Betti, F. Bussolotti, V. Carravetta, U. Ekström, C. Mariani, and S. Stranges, J. Chem. Phys. **122**, 124305 (2005).
[12] N. Kosugi, J. Electron Spectrosc. Relat. Phenom. **137-140**, 335 (2004).
[13] H. J. Aa. Jensen, T. Saue, L. Visscher, with contributions from Bakken, E. Eliav, T. Enevoldsen, T. Fleig, O. Fossgaard, T. Helgaker, J. Laerdahl, C. V. Larsen, P. Norman, J. Olsen, M. Pernpointner, J. K. Pedersen, K. Ruud, P. Salek, J. N. P. van Stralen, J. Thyssen, O. Visser, and T. Winther, Computer code DIRAC, 2004.
[14] J. Olsen and P. Jørgensen, J. Chem. Phys. **87**, 3235 (1985).
[15] U. Kaldor and S. Wilson, *Theoretical Chemistry and Physics of Heavy and Superheavy Elements* (Kluwer Academic Publishers, Dordrecht, 2003).
[16] M. H. Mittleman, Phys. Rev. A **24**, 1167 (1981).
[17] T. Saue and H. J. Aa. Jensen, J. Chem. Phys. **111**, 6211 (1999).
[18] G. Herzberg, *Molecular Spectra and Molecular Structure III: Electronic Spectra and Electronic Structure of Polyatomic Molecules* (Von Nostrand Reinhold Company, New York, 1966).
[19] D. Woon and T. Dunning, Jr., J. Chem. Phys. **98**, 1358 (1993).
[20] R. E. LaVilla, J. Chem. Phys. **62**, 2209 (1975).
[21] S. Svensson, A. Ausmees, S. J. Osborne, G. Bray, F. Gel'mukhanov, H. Ågren, A. Naves de Brito, O.-P. Sairanen, A. Kivimäki, E. Nõmmiste, H. Aksela, and S. Aksela, Phys. Rev. Lett. **72**, 3021 (1994).
[22] E. Hudson, D. A. Shirley, M. Domke, G. Remmers, and G. Kaindl, Phys. Rev. A **49**, 161 (1994).
[23] M. R. F. Siggel, C. Field, K. J. Borve, L. J.Sæthre, and D. T. Thomas, J. Chem. Phys. **105**, 9035 (1996).
[24] A. Naves de Brito and H. Ågren, Phys. Rev. A **45**, 7953 (1992).
[25] W. Schwarz, Chem. Phys. **11**, 217 (1975).
[26] M. Robin, Chem. Phys. Lett. **31**, 140 (1975).
[27] I. Cacelli, V. Carravetta, and R. Moccia, Chem. Phys. **120**, 51 (1988).